INDIAN JOURNAL OF SCIENCE AND TECHNOLOGY

RESEARCH ARTICLE

Designing of Unit EBG Cell Using Conductive Textile for Dual Band Operation

Sangeeta Shekhawat[1]*, Sudhanshu Singh[1], Sanjay Kumar Singh[1]

1 Amity School of Engineering & Technology, Amity University Rajasthan, Jaipur303002, NH11 C, Jaipur, Kant Kalwar, Rajasthan, India

OPEN ACCESS

Received: 01-12-2022

Accepted: 13-04-2022

Published: 25.05.2022

Citation: Shekhawat S, Singh S, Singh SK (2022) Designing of Unit EBG Cell Using Conductive Textile for Dual Band Operation. Indian Journal of Science and Technology 15(18): 881-891. https://doi.org/10.17485/IJST/v15i18.1843

* **Corresponding author**.

*sangita_shekhawat@yahoo.com

Funding: None

Competing Interests: As a non-financial conflict of interest, the paper titled ' conductive textile EBG unit cell AMC surface analysis for 2.45ghz and 5.5ghz band of frequencies ' was submitted to ' Journal of Hunan University Natural Science,' on the August Month 2021. At the time of submission, we have not checked the authenticity of that journal. Soon we caught that thing on Clone I/II link on UGC CARE site. I along with my co-authors have written a withdrawal email to the editor. This paper is not submitted anywhere except IJST.

Published By Indian Society for Education and Environment (iSee)

ISSN
Print: 0974-6846
Electronic: 0974-5645

Abstract

Background/Objectives: Flexible electronics have paved the way for Wireless Body Area Networks (WBAN). The main challenge in accommodating such applications is reducing the impact of radiation on the human body. The presence of body tissues may affect WBAN devices such as wearable sensors and wearable antennas, so reducing back radiations becomes an important task. **Methodology:** When a microstrip patch antenna is placed on a human body, the artificially formed Electromagnetic Band Gap (EBG) surface mimics the property of a Perfect Magnetic Conductor (PMC) rather than the conventional Perfect Electrical Conductor (PEC). **Findings:** In this work, the unique property of the EBG surface beneath the patch antenna creates a zero phase shift at the resonance, which improves the antenna's performance and reduces back radiations as well. The proposed EBG surface structure is the simplest square-shaped structure with no conductor connections Via patch (Via-less). **Novelty:** The EBG structure designed and presented in this paper has zero reflections for the dual-band of operations. The resonance frequency of 2.45GHz and 5.5 GHz has been designed for the absorption of 80% and 65% respectively. This level of absorption has not yet been reported in the literature. The newly formed EBG cell integrated with the patch antenna and its performance improvements has been shown. The analysis shows that the EBG enhances the return loss by 20.35 % and gain enhances by 16.44 %, on textile materials with the advantage of most simplex EBG cell construction.

Keywords: EBG; PMC; PEC; Wearable Microstrip Patch Antenna; WBAN

1 Introduction

Recent advancements in the field of flexible electronics are opening the doors for various emerging fields. The body-worn applications of wireless communication may lead to performance degradation due to the close vicinity of the human body[(1)]. This makes it necessary to take a detailed study on the flexible antenna concerning Specific Absorption Rate (SAR), which shows the absorption of heat of radiation by human body tissues[(2)]. Artificial Magnetic Conductor (AMC) structure is not found naturally

but they are designed artificially. These structures possess the unique properties of Electromagnetic (EM) waves. The property of AMC could also be used to improve the performance of wearable devices when they are being worn on the human body. The vast and unique property of AMC is used to mimic the property of PMC for wireless communications not only in wearable systems. The AMC can be configured to function as a bandpass or band stop filter. The presence of the human body in the wearable microstrip patch antenna application changes the performance parameters as well as generates back radiation, which is then absorbed by the human body tissues [(2)]. In this work, the property of AMC has been used to mimic the property of the Perfect Magnetic Conductor (PMC). A fully textile-based EBG Cell structure is designed in the simplest way possible, with no Via used for dual-band operation.

The work reported earlier was too thick to integrate with a lightweight, flexible form, so cannot withstand several bending [(3–10)]. Bending analysis has been done in some semi textile antennas they are providing the poor Front to Back Ratio (FBR) [(11–16)]. The EBG structure designs have previously been demonstrated in [(2,3,5,8,9)] patch antenna works. Though initially in [(17)] the EBG structure was simpler it is using a Via between the EBG cell and ground. The Bandgap feature was added to the literature with the help of Via. However, the Vias could be used to control the effective inductance, the risk of manufacturing inaccuracy is always higher because of the textile materials. In the same work author tries to simply the EBG cell structure by making the Via-less EBG Cell, so the effective inductance must be increased. To increase the effective inductance the author has made a complex cut inside the EBG cell to form the 2 x 2 EBG structure. The present reported work has the simplest EBG structure without using any Vias, this Via-Less EBG structure is also easy to fabricate in textile materials. The primary goal of this work is to design the simplest EBG cell with dual-band operation using textile materials. Absorption, reflections, and band stop bandwidth are all thoroughly discussed.

The major goal of this work is to form the simplest EBG cell with dual-band operation with textile materials, the absorption, reflections, and the band stop bandwidth are discussed further. The proposed EBG cell providing the band gap for the 2.45 GHz standard Industry, Scientific and Medical band (ISM) of applications and 5.5 GHz, Worldwide Interoperability for Microwave Access (WiMAX) band of IEEE 802.16. This band is used for wireless data over long distances in a variety of ways, from point-to-point links to full mobile cellular type access. The selection of these two bands were based on the demand of emerging devices of wireless devices works on ISM and WiMAX band. The wireless devices become an integral part of our daily life now a days. Integration of technology such as WLAN, WiMAX, Bluetooth, and others into a single handheld device has shown to be an excellent way to boost commercial progress.

2 Material and Methods

The wearable antenna must be entirely textile-based and provide continuous information about the wearer's health/communication signals. As a result, the need for two distinct textiles arises. One is non-conducting for the substrate and the other is conducting for EM wave radiation. The conducting textile materials, also known as electro textile, make the wearer comfortable while communicating information. Because textile antennas must be placed on the human body, the efficiency of the antenna is drastically reduced due to the lossy nature of human tissue. When a textile antenna is placed close to the human body, the dielectric constant of the substrate textile is affected, which may reduce the radiation characteristics and, as a result, changes other parameters such as S_{11} (return loss), VSWR (Voltage Standing Wave Ratio), Gain, Radiation Patterns etc.

Various textile fabrics, such as fleece, silk, flannel, wool, polyester, denim, Cardura, and felt, are used as substrates in the literature [(18)]. Conducting patch fabrics include ShieldiT, copper sheet, Zelt, flexion, and pure copper taffeta.

This AMC structure could also be used to improve radiation properties while minimizing backward radiation to the human body. The whole combination makes this structure more popular among antenna designers. The resonance frequencies and bandwidth of this AMC reflector structure are significantly affected by the unit cell geometry, dielectric property, and substrate thickness [(4)].

In this paper dielectric fabric, Felt is used as the substrate of antenna which is the non-conductive substrate. Shieldit Super conductive textile is used to form the unit cell and conductive ground.

Shieldit Super conducting textile is a soft but strong polyester substrate that has been copper and nickel plated. This fabric has one side coated with a non-conductive hot melt adhesive, which aids in the attachment process in this work by ironing the conducting fabric on top of the felt substrate textile. With a thickness of 2.5 mm, felt has a dielectric constant of 1.36, a loss tangent of 0.023, and a dielectric constant of 1.36. Shieldit Super is 0.15 mm thick and has a conductivity of 6.67 x 10^5 S/m.

There have been reports of various shapes and designs that could be used as the Unit cell geometry to create the band stop or bandpass surface structure. The Square shaped structure is used in this proposed work to form the High Impedance Surface (HIS) for the application of 2.45 GHz and 5.5 GHz resonance frequency bands.

The dimensions of the square shape are taken from their parametric analysis report, which is included in this study. The unit cell response has a good bandwidth for both above-mentioned frequency bands. The selection of conductive textile is critical because it must be worn on the human body while also radiating signals. Because the electrical properties of elastic materials change when bent, this fabric should be inelastic. To minimize losses, the material must also be homogeneous across the antenna area, with a minimal difference in resistance through the material.

2.1 Properties of EBG Unit Cell

The HIS property is important in the design of the EBG surface because surface waves occur whenever two dissimilar media are used for propagation. Surface waves are electromagnetic waves that propagate in an exponential fashion into the surrounding space. The EBG structure is used to prevent the surface waves from being produced by dissimilar media, leading to minimal antenna backward radiations. Consequently, the amount of energy wasted in the undesired (here backward for microstrip patch antenna) direction is reduced. Surface wave propagation is normally parallel to the interface and decreases exponentially away from it. The inductive surface support Transverse Magnetic (TM) surface waves, while the capacitive surface support Transverse Electric (TE) surface waves as represented in (1) and (2) respectively.

$$Zs(TM) = j\alpha / \omega\varepsilon \quad (1)$$

$$Zs\ (TE) = -j\omega\mu/\alpha \quad (2)$$

Where ω is the angular frequency (rad/sec), ε is the dielectric permittivity (F/m), μ is the permeability (Wb/Amp) and α is the propagation constant.

The impedance vs. frequency relationship of HIS at low frequency the impedance is inductive and at high frequency the characteristic is capacitive. So below the reference it supports the TM surface waves and above the resonance it supports the TE waves. At the resonance it exhibits high/ infinite as could be calculated by the equation.

$$Z(\omega) = j\omega L/1 - 2\omega LC \quad (3)$$

It demonstrates that it does not support any surface wave at resonance. This is the most important property of HIS, and it is used as a conducting surface for the patch ground where back radiations have a negative effect on the human body for wearable applications. When radiations are placed close together, the human body behaves like a lossy dielectric medium, affecting performance parameters significantly. Another important property of HIS is its dual to PEC capability (Perfect electric conductor). The perfect electric conductor (PEC) has abounded electrons, and when an electric field is applied to the PEC surface, these electrons become excited and generate the surface current surface impedance is ideally zero, and it does not support any electric field inside the conductor; any radiation that strikes on its surface is, reflected by 180^0 phase. When the impedance is exceptionally low (practically) in comparison to the free space impedance, as in

$$\Phi = \pm \pi \quad (4)$$

When it matches the free space impedance it is equivalent to

$$\Phi = \pm \pi/2 \quad (5)$$

When the impedance becomes high, the phase becomes zero, which is at resonance where the reflection phase is zero.

It also has the property to block the electric field and no electric field can penetrate the surface. The counterpart of PEC is the Perfect Magnetic Conductor (PMC) this is not naturally formed this is a designed and conceptualized surface that can block magnetic fields instead of electric. As compared to the PEC the PMC surface impedance Zs is extremely high, and it is not present in any natural material, but the property of PMC can be mimicked in the form of artificially formed sheets where different techniques are used to show the above-mentioned property of PMC.

AMC is a type of PMC, by using the periodic arrangement of identical or similar structures the property of magnetic conductor could be introduced in this PMC sheet. Broadly the AMC, FSS (Frequency Selective Surface), and SRR (Slip Ring Resonator) all come under the Metasurface/ Metamaterial. So, AMC is the subpart of Metamaterial. It is most important to know the property of this PMC surface. Figure1(a) shows the basic property of PEC and AMC surface that when any incident wave strikes on the PEC surface after reflection the phase of reflected wave shifts by 180^0 but when the wave reflects the AMC surface the reflected wave does not shift the phase of the incident wave. It shows that AMC does not invert the phase of the incident input signal. So, to enhance the performance of the patch antenna and to reduce the back radiation this AMC surface has vast applications.

Figure 1(a) depicts the basic property of the PEC and AMC surfaces: when an incident wave strikes the PEC surface after reflection, the phase of the reflected wave shifts by 180^0, whereas when the wave reflects the AMC surface, the reflected wave does not shift the phase of the incident wave. It shows that AMC does not invert the phase of the incident input signal. As a result, this AMC surface has a wide range of applications for improving patch antenna performance and reducing back radiation.

Figure 1 shows the concept of surface current before and after the AMC surface (a). In the microstrip patch antenna, the current in the patch and current in the metal ground part are out of phase, but if the AMC sheet is replaced instead of the metal

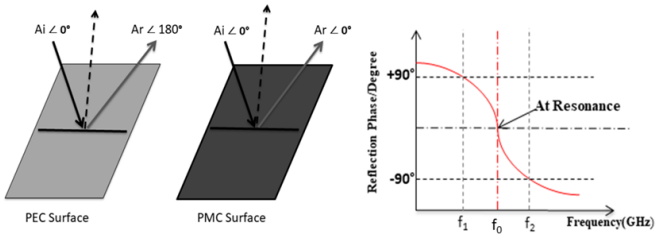

Fig 1. (a) PEC and AMC surface basic property (b) Bandwidth of the AMC surface structure resonating at f0

PEC ground, the phase shift is reduced to zero. After reflecting from the AMC surface, both the incident and reflected waves will be in the same phase.

To calculate the absorption of surface waves, the bandwidth of the AMC surface must first be calculated. The bandwidth of this AMC is defined as the difference between two frequencies when they pass the reflection phase/degree by $+90^0$ to -90^0 [(5)].

Numerous studies are being conducted on such artificially formed conductors and used as bandwidth enhancers for microstrip patch antenna [(6,7)]. Electromagnetic waves and their backscattering are controlled by such AMC surfaces which are demonstrates as the reflective Metasurface [(8,11)].

Figure 1(b) displays the AMC surface's bandwidth, where the frequency at which the reflection phase is zero is known as the resonance frequency. The surface will exhibit the property of a two-dimensional electric filter for a specific frequency range at this resonance frequency. The two frequencies f_1 and f_2 show the bandwidth of AMC or the stop band frequency range before and after the resonance in this band, the equivalent LC network acts as a band stop filter to restrict the flow of surface waves. The AMC will not invert the phase of the reflected wave within this frequency range.

2.2 Design and Parametric Analysis of Unit EBG Cell

Apply the concept of reflection, the geometry for this reflecting surface must be developed. The TM wave can only travel through an inductive surface, whereas TE wave can only pass through a capacitive surface. Special artificially formed surface structures with inductive and capacitive surface impedance must be developed to prevent the propagation of both TM and TE surface waves. This is an example of an LC resonance structure. Surface waves can be avoided by texturing the surface with periodic lumped element resonance structures over a finite frequency range. Radiation interference prevents surface waves from propagating as they scatter from the discontinuity, resulting in a large impedance bandgap over the frequency range. A periodic structure could be generated by cascading the two-port network into unit cells.

Its features are described using effective surface models. These devices are usually made up of a lumped inductance and a capacitance, and they have high impedance in a specific frequency band. To absorb the back radiations generated by the microstrip patch antenna, a variety of periodic similar structures have been investigated and simulated.

In Figure 2(a), the unit EBG cell design is shown, this is designed and simulated in Ansys HFSS simulator. The unit EBG Cell dimensions taken for parametric analysis are S_1 and S_2 from 30 mm to 31 mm, P_1 and P_2 from 28 mm to 29 mm, C_1 and C_2 from 20 to 21 mm, and I_1 and I_2 kept constant at 19 mm. By varying the dimensions of the outer patch (P_1 and P_2) along with S_1 (dimension of the unit cell), cuts (C_1 and C_2), and keeping the inner patch (I_1 and I_2) constant the required Bandgap for 2.45 GHz and 5.5 GHz could get. The EBG Bandgap bandwidth has been taken between $\pm 90^0$.To analyses, the EBG unit cell Floquet port is used in Ansys HFSS simulator [(12)].

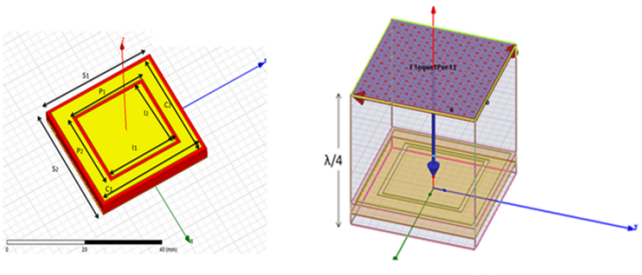

Fig 2. (a) Unit EBG Cell with dimension parameters (b) EBG Unit Cell with Floquet Port

Floquet port is shown in Figure 2(b), the distance from the top of the patch is taken as $\lambda/4$ for the case of Floquet port to check the reflection phase/degree in the analysis of unit cell geometry. For the simulation of the unit cell, the boundaries must be decided. There are two models popular by which the boundary condition could be defined, here in this work the Master and Slave boundaries are defined, the direction of the respective master and slave must be assigned in the same direction.

2.3 Designing of Microstrip Patch Antenna

The demand of microstrip patch antennas is increasing day by day because it could be directly printed on the circuit board. It is also very popular because of its simple design, easy handling, compact size, economical for mass fabrication etc. The major disadvantage of such printed antennas are their low gain and directivity. The EBG structure presented in previous section designed to improve the performance of the patch antenna, especially when it must be used for the Body Worn Applications.

The patch antenna comprises one dielectric substrate on which one side is covered with conducting ground and other side having the radiator patch. The dielectric substrate is sandwiched between two conducting sheets. For the designing of textile-based antenna the dielectric and conductive both surfaces must be textile. In the proposed work the radiating patch and ground both formed by the conductive ShieldiT textile and for the dielectric substrate Felt textile is used which is like the EBG cell material. The patch antenna's dimensions are calculated, and the final dimensions are used for simulation work after a parametric study [24].

In Figure 3(a), the patch antenna final dimensions are shown the quarter wave transformer section is used to match the impedance of the antenna. The (a) is the basic antenna without EBG Cell surface and in Figure 3(b) the EBG integrated patch is depicted.

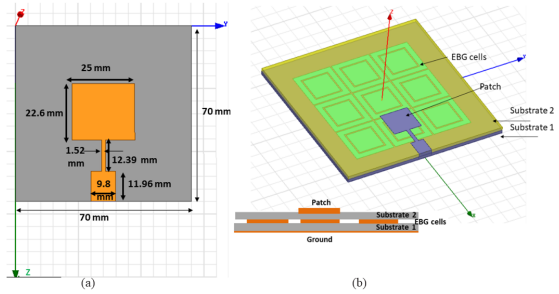

Fig 3. (a) Dimensions of patch antenna without EBG Surface (b) Patch antenna integrated with EBG Surface(EBG Cells sandwiched between the two substrates.)

3 Results and Discussion

Parametric study reveals the exact dimensions at which the desired resonance bands will give the band stop performances. The desired bands are standard 2.45 GHz and 5.5 GHz frequencies.

As shown in Figure 4(a) and Figure 4(b), the samples the dimensions of the unit cell and its parametric run. The basic dimension of the unit cell was taken from the literature used in the ISM band.

This dimension was calculated by using the Sievenpiper's Equations, but it must be optimized through parametric analysis. The various dimensions of the unit cell are shown in Figure 4(a) and sample no 43 gives the optimized value of the desired band of operation.

Table 1 shows the variables of the unit cell and the final selected values for the EBG surface. The value of I1 and I2 kept constant. As we are increasing the gap between two squares in the EBG cell the capacitance will increase and when the length of EBG increases then the inductance of the periodic structure increases based on the parametric analysis we have the zero reflection at resonance frequency 2.45 GHz and 5.5 GHz.

Dual Band Operation

In [18], author designed EBG plane is providing the effect of AMC substrate only for one frequency band of 5.4GHz. The patch antenna is designed to resonate on 2.45 GHz so, for the patch resonance frequency the EBG plane behaves like a normal PEC but when the antenna resonates on its second band (5.4 GHz) then the EBG substrate plays a role as to reduce the back radiation.

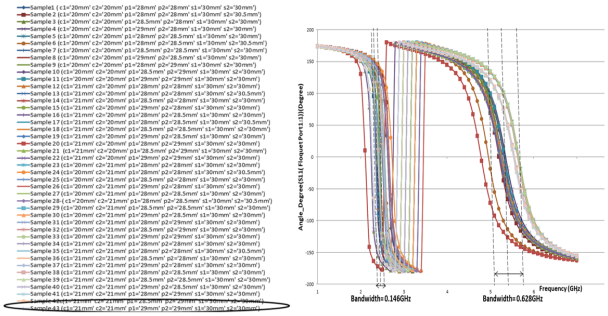

Fig 4. (a) Various sample dimensions for parametric analysis (b) Simulation result of parametric analysis of Unit EBG Cell

Table 1. Parameters Used for Parametric Analysis

S.no	Variable parameters(mm)	Range of Variables	Final Selection
1	S_1	30 mm to 31mm	30 mm
2	S_2	30 mm to 31 mm	30mm
3	P_1	28 mm to 29 mm	29 mm
4	P_2	28 mm to 29 mm	29 mm
5	C_1	20 mm to 21 mm	21 mm
6	C_2	20 mm to 21 mm	21 mm

The EBG plane works as the reflector and does not excite the parallel plate mode in between the antenna plane and ground plane. The reflection and absorption properties of EBG are also very important to study, in the [18] author has not provided the absorption and reflections of the EBG surface.

The major achievement in this newly presented work is dual-band operation for which the EBG plane approaches as the PMC, as well as absorption and reflection for dual bands, are also explained. Figure 5(a) shows the finding of the present work where the two shaded areas show the two resonances over which the phase is zero. The EBG structure bandwidth is the frequency range within which the reflection phase changes from $+90^0$ to -90^0, as shown in (a). The two red shaded areas in this case indicate that the resonant frequencies of 2.45 GHz and 5.5 GHz are at zero reflection phases. The primary goal of this work is to appropriately design the patch size so that the antenna resonant frequency drops within the EBG band gap, thereby prohibiting surface waves. This designed antenna's resonance frequency can be covered by the EBG band gap. The EBG bandwidth is depicted in Figure 5(c), with the first band width ranging from 2.404 GHz to 2.55 GHz and the second band width ranging from 5.227 GHz to 5.855 GHz. The results of [18] as shown in Figure 5(b) it has only one resonance at which phase is zero.

The design structure of EBG cell in Figure 5(d) simulated and implemented in [19] to get the dual band of operation. There are some dual bands EBG performance is being reported in literature, but when the based and conductive material is textile than the design of EBG cell must play a key role. As shown in Figure 5(d) and (e) the EBG presented is not much simple to cut into a textile design. The proposed EBG cell in this work is extremely simple to cut without any deformation in their structure. The bandwidth is calculated by the upper frequency, lower frequency, and resonance frequencies as shown in Figure 5(c). The bandwidth for 2.45GHz resonance is 0.146 GHz and for 5.5 GHz is 0.628 GHz. This becomes the major finding of this work that a single EBG plane surface will work for both the applications of ISM 2.45 GHz band as well as 5.5 GHz, WiMAX applications.

In Figure 6(a) the reflection of the wave is plotted with the absorption for the desired band of 2.45 GHz and 5.5 GHz. The absorption is around 80 % and 65% for 2.45 GHz and 5.5 GHz respectively, which is comparatively fair when the textile material is used. The designing of textile patch antenna may become complex if the EBG cells are complicated, so simple square shaped EBG cells are providing better results with ease in designing. (b) represents the magnitude and phase comparison for desired bands of operation.

In Figure 7, surface current distribution is represented on both the resonance frequencies. In Figure 7(a), shows the surface current when adaptive pass resonance frequency is being set at 2.45 GHz with 0^0 phase angle, (b) represents when the phase is shifted to 30^0.Figure 7(c) and (d) represents the surface current distribution at 5.5 GHz frequency with 0^0 and 30^0respectively.

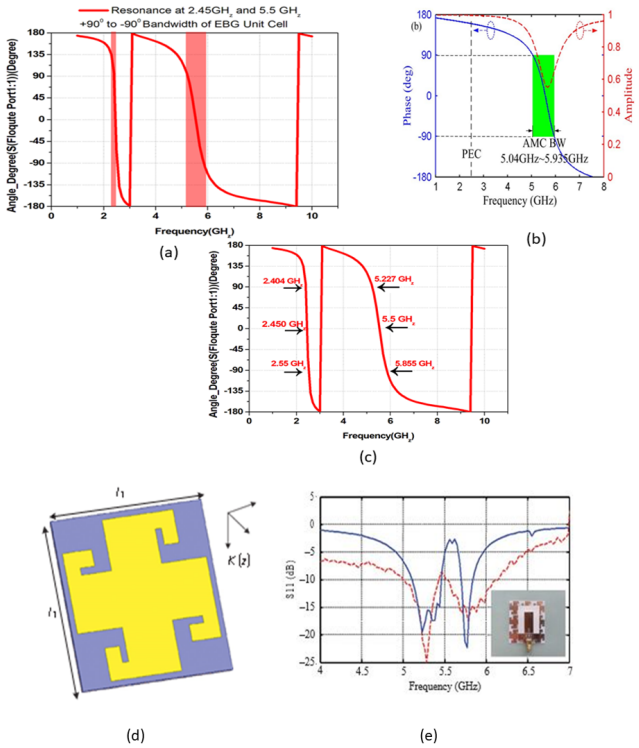

Fig 5. (a) AMC Dual bandwidth between $\pm 90^0$ at resonance at 2.45GHz and 5.5 GHz in proposed work (b) The single EBG Bandwidth at resonance 5.4 GHz [18] (c) Finally selected EBG Unit cell results for both resonances along with their bandwidth in proposed work (d) The dual band EBG cell [19] (e) The dual band EBG cell integrated with Patch antenna in literature [19]

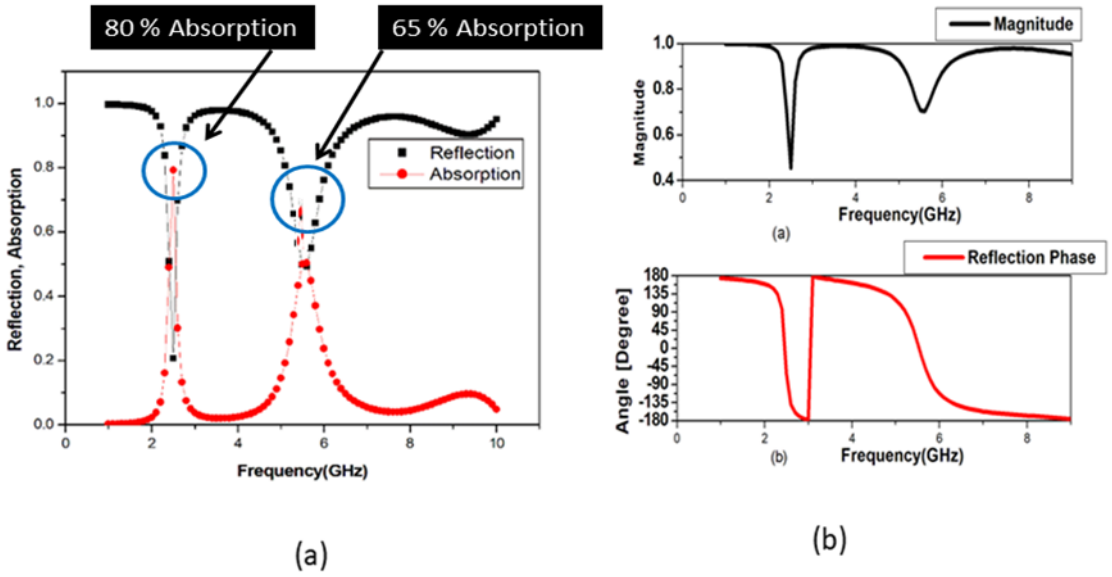

Fig 6. (a) The reflection and Absorption for the desired dual band operation (b) Magnitude levels of EBG Cell with respect to their angle (degree)

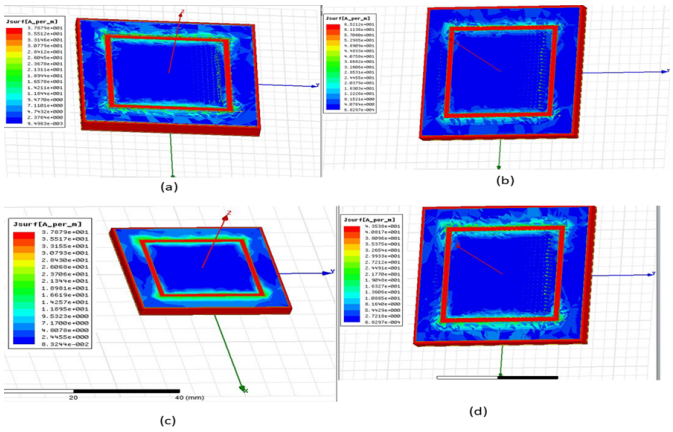

Fig 7. Surface current distribution in EBG Unit cell (a) For the 2.45 GHz and 0^0 phase, (b) 2.45 GHz 30^0phase, (c) 5.5 GHz with 0^0 phase, (d) 5.5 GHz 30^0 phase

In Figure 8, the dispersion of unit EBG cell is represented. The EBG does not permits to flow the surface waves for specific frequency. The proposed EBG cell would not permit to flow the surface wave s between the range of 2. 404 GHz to 2.55 GHz and 5.227 GHz to 5.855 GHz frequencies. These two bands stop width is represented in Figure 8. For the measurement of dispersion, the EBG cell is simulated in Eigen-Mode solution type in the Anys HFSS simulator. The proper selection of Unit cell boundaries the structure would behave like an infinite structure. Dispersion diagram plotting requires three sets of simulations. These three sets of simulation consist unique phase shifts. First part is in x- boundary plane shift from 0^0 to 180^0, which is represented in Figure 8 from Γ to X direction, for this simulation the Y axis is fixed at 0^0.This is also known as Γ to X Plot.

The Third part is between M to Γ part, both X and Y axis boundaries phase shift will be shifted from 0^0 to 180^0 at the same time.

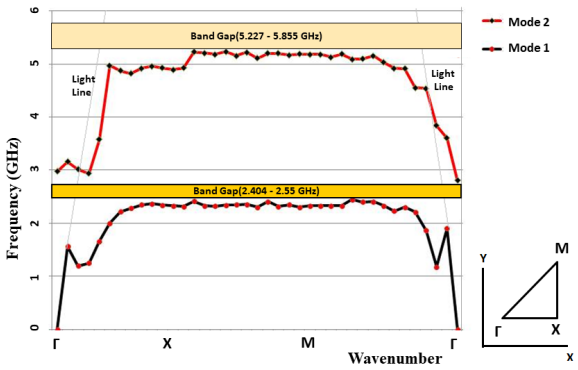

Fig 8. Dispersion diagram for EBG cell structure

In Figure 9 (a), the complete EBG cell-based AMC surface is shown, where the ground and EBG Cells are formed using Shieldit Super textile (Yellow) and the dielectric substrate is Felt textile (Red). This surface will behave like a PMC and will not change the phase of reflected wave and absorption the radiations on the backside for both the resonance frequencies.

This artificially formed PMC will be best for body-worn applications it will protect the human tissues to absorb the radiation from the radiating patch.

Performance Enhancement of Microstrip Patch Antenna with the EBG Surface

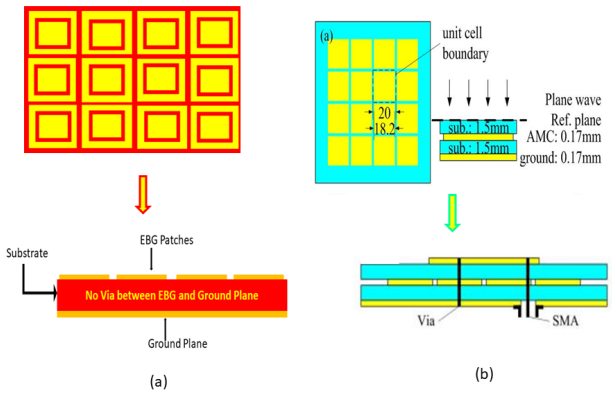

Fig 9. (a) Complete AMC 3 x4 EBG cell surface for proposed work and (b) Via-Based EBG in reference [18]

The EBG surface is now integrated with a microstrip patch antenna, where it is supposed to be absorbing the surface waves and therefore the performance characteristics will be tested. The patch antenna's major characteristics are Return loss also known as Scattering parameters S_{11}, Radiation pattern, Gain, 3-D polar plots, etc. In this work, the important parameters are compared with and without the EBG integration.

Return Loss

Return loss is the measure of the power reflected by the source due to discontinuities and mismatches. So, it becomes the major performance parameter that gives the measure of how well the device is matched with other devices for communication. As the plot is shown in Figure 10(a) the value of the return loss(S_{11}) has been improved from -24.18707 dB to -29.109 dB at the resonance frequency of 5.5 GHz. The patch antenna will be useful when it is greater than -10 dB.

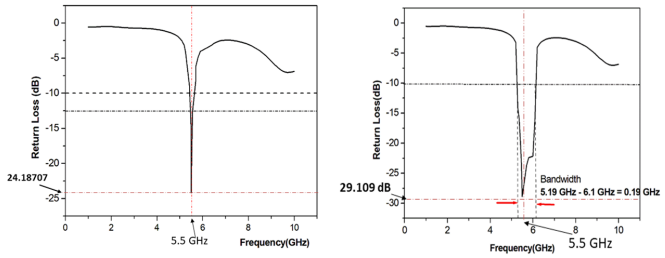

Fig 10. (a) The return loss of the patch antenna without EBG Surface and (b) Return loss with EBG

Radiation Pattern

The radiation pattern of a microstrip patch antenna is a graphical representation of the energy radiation in space. Figure 11(a) and (b) show the pattern of the proposed patch with and without EBG. The pattern is commonly referred to as the Azimuth and Elevation plane pattern. The pattern lobe represents the energy radiation; a lobe is any part of the pattern that is surrounded by weaker radiations. As a result, it is known as the major lobe and the side lobes. The major lobe is responsible for most radiations, and side lobes are unnecessary, even though they waste radiation energy. The radiation pattern of a Microstrip patch antenna without EBG is depicted in Figure 11(a), where the major radiations occur in the + Z direction but the main lobe is not much confined in this direction, and the energy is also radiating in the backward direction represented by the back lobes. Figure 11(c) and (d) show 3-D plots of far field radiations. Polar plots depict the distribution of radiation energy with respect to the directional coordinator without and with the EBG.

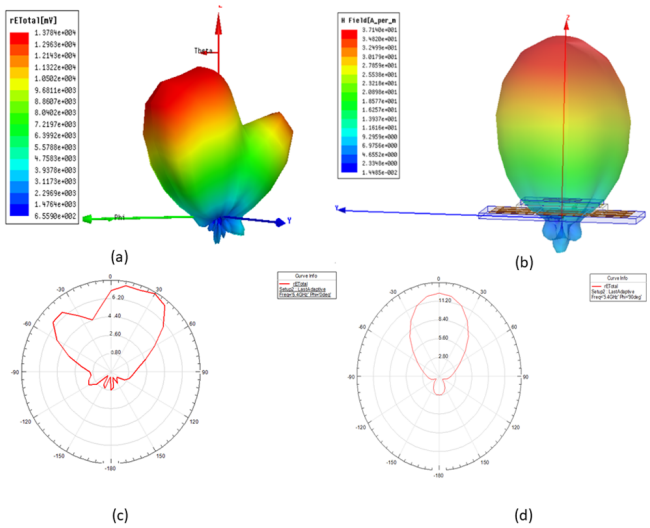

Fig 11. (a) Radiation Pattern without EBG and (b) Radiation pattern of the antenna with EBG surface (c) 3-D Polar Plot of antenna without EBG AND (d) 3-D polar plot of the antenna with EBG surface

Gain

Gain is the key performance characteristic of any radiator, which combinedly represents the antenna's directivity as well as radiation efficiency. The larger the value of gain signifies more capability to radiate the energy by the radiator. For the microstrip patch antenna, the gain is frequency dependent parameter. The gain for the proposed antenna design is 6.09 dB as shown in Figure 12(a) when the EBG surface is not added. The gain has been improved from 6.09 to 7.0914 dB.

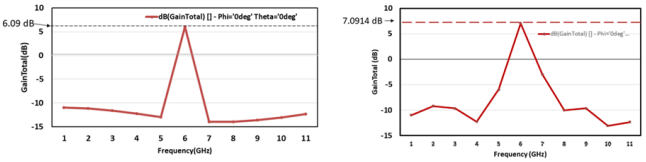

Fig 12. (a) Gain Vs Frequency plot of antenna without EBG and (b) Gain Vs. Frequency plot of the antenna with EBG Surface

4 Conclusion

The Shieldit Superconductive textile and Felt-based designed AMC surface dual-band absorption will be best suited for the 2.45 GHz and 5.5 GHz range of frequencies. The simulation result shows that this surface will be best for the absorption of the back radiation in both the resonance frequency bands. The key point of this work is the simplex Via-less design of EBG cells so, they could be easily fabricated on any type of textile. Shieldit Super textile is coated with non-conductive hot melt adhesive on one side. This makes the attachment process easier by ironing the conducting fabric on the top of the textile felt substrate in this proposed work. The surface shows 80% absorption for the 2.45 GHz ISM band and 65 % absorption for the 5.5 GHz frequency, which is not yet been reported in the simplest square EBG Cell structure. To check the performance enhancement of the microstrip patch antenna the newly designed EBG surface is integrated with the patch antenna resonation at the 5.5 GHz band of frequency. The analysis shows that the EBG enhances the return loss by 20.35 % and gain enhances by 16.44 %, on textile materials with the advantage of most simplex EBG cell construction.

References

1) Atrash ME, Abdalla MA, Elhennawy HM. A compact flexible textile artificial magnetic conductor-based wearable monopole antenna for low specific absorption rate wrist applications. *International Journal of Microwave and Wireless Technologies*. 2021;13(2):119–125. Available from: https://dx.doi.org/10.1017/s1759078720000689.

2) Ashyap AYI, Abidin ZZ, Dahlan SH, Majid HA, Kamarudin MR, Alomainy A, et al. Highly Efficient Wearable CPW Antenna Enabled by EBG-FSS Structure for Medical Body Area Network Applications. *IEEE Access*. 2018;6:77529–77541. Available from: https://dx.doi.org/10.1109/access.2018.2883379.
3) Ashyap AYI, Dahlan SHB, Abidin ZZ, Dahri MH, Majid HA, Kamarudin MR, et al. Robust and Efficient Integrated Antenna With EBG-DGS Enabled Wide Bandwidth for Wearable Medical Device Applications. *IEEE Access*. 2020;8:56346–56358. Available from: https://dx.doi.org/10.1109/access.2020.2981867.
4) Potey PM, Tuckley K. Design of wearable textile antenna for low back radiation. *Journal of Electromagnetic Waves and Applications*. 2020;34(2):235–245. Available from: https://dx.doi.org/10.1080/09205071.2019.1699170.
5) Ashyap AYI, Abidin ZZ, Dahlan SH, Majid HA, Saleh G. Metamaterial inspired fabric antenna for wearable applications. *International Journal of RF and Microwave Computer-Aided Engineering*. 2019;29(3):e21640–e21640. Available from: https://dx.doi.org/10.1002/mmce.21640.
6) Sanchez-Montero R, Camacho-Gomez C, Lopez-Espi PL, Salcedo-Sanz S. Optimal Design of a Planar Textile Antenna for Industrial Scientific Medical (ISM) 2.4 GHz Wireless Body Area Networks (WBAN) with the CRO-SL Algorithm. *Sensors*. 1982;18(7):29933585–29933585.
7) Sanchez-Montero, Lopez-Espi, Alen-Cordero, Martinez-Rojas. Bend and Moisture Effects on the Performance of a U-Shaped Slotted Wearable Antenna for Off-Body Communications in an Industrial Scientific Medical (ISM) 2.4 GHz Band. *Sensors*. 2019;19(8):1804–1804. Available from: https://dx.doi.org/10.3390/s19081804.
8) Bait-Suwailam MM, Labiano II, Alomainy A. Impedance Enhancement of Textile Grounded Loop Antenna Using High-Impedance Surface (HIS) for Healthcare Applications. *Sensors*. 2020;20(14):3809–3809. Available from: https://dx.doi.org/10.3390/s20143809.
9) Gao G, Wang S, Zhang R, Yang C, Hu B. Flexible EBG-backed PIFA based on conductive textile and PDMS for wearable applications. *Microwave and Optical Technology Letters*. 2020;62(4):1733–1741. Available from: https://dx.doi.org/10.1002/mop.32224.
10) Atrash ME, Abdalla MA, Elhennawy HM. A Compact Highly Efficient Π-Section CRLH Antenna Loaded With Textile AMC for Wireless Body Area Network Applications. *IEEE Transactions on Antennas and Propagation*. 2021;69(2):648–657. Available from: https://dx.doi.org/10.1109/tap.2020.3010622.
11) Guan CE, Fujimoto T. Design of a Wideband L-Shape Fed Microstrip Patch Antenna Backed by Conductor Plane for Medical Body Area Network. *Electronics*. 2019;9(1):21–21. Available from: https://dx.doi.org/10.3390/electronics9010021.
12) Elfergani I, Iqbal A, Zebiri C, Basir A, Rodriguez J, Sajedin M, et al. Low-Profile and Closely Spaced Four-Element MIMO Antenna for Wireless Body Area Networks. *Electronics*. 2020;9(2):258–258. Available from: https://dx.doi.org/10.3390/electronics9020258.
13) Ullah M, Islam M, Alam T, Ashraf F. Paper-Based Flexible Antenna for Wearable Telemedicine Applications at 2.4 GHz ISM Band. *Sensors*. 2018;18(12):4214–4214. Available from: https://dx.doi.org/10.3390/s18124214.
14) Gao GP, Hu B, Wang SF, Yang C. Wearable Circular Ring Slot Antenna With EBG Structure for Wireless Body Area Network. *IEEE Antennas and Wireless Propagation Letters*. 2018;17(3):434–437. Available from: https://dx.doi.org/10.1109/lawp.2018.2794061.
15) Joshi R, Hussin EFNM, Soh PJ, Jamlos MF, Lago H, Al-Hadi AA, et al. Dual-Band, Dual-Sense Textile Antenna With AMC Backing for Localization Using GPS and WBAN/WLAN. *IEEE Access*. 2020;8:89468–89478. Available from: https://dx.doi.org/10.1109/access.2020.2993371.
16) Azeez H, Yang HC, Chen WS. Wearable Triband E-Shaped Dipole Antenna with Low SAR for IoT Applications. *Electronics*. 2019;8(6):665–665. Available from: https://dx.doi.org/10.3390/electronics8060665.
17) Ashyap AYI, Elamin NIM, Dahlan SH, Abidin ZZ, See CH, Majid HA, et al. Via-less electromagnetic band-gap-enabled antenna based on textile material for wearable applications. *PLOS ONE*. 2021;16(1):e0246057–e0246057. Available from: https://dx.doi.org/10.1371/journal.pone.0246057.
18) Zhang K, Soh PJ, Yan S. Meta-Wearable Antennas—A Review of Metamaterial Based Antennas in Wireless Body Area Networks. *Materials*. 2020;14(1):149–149. Available from: https://dx.doi.org/10.3390/ma14010149.
19) Mu G, Ren P. A Compact Dual-Band Metasurface-Based Antenna for Wearable Medical Body-Area Network Devices. *Journal of Electrical and Computer Engineering*. 2020;2020:1–10. Available from: https://dx.doi.org/10.1155/2020/4967198.